

## Making the most out of the least (squares migration)

Gaurav Dutta, Yunsong Huang, Wei Dai, Xin Wang, and G.T. Schuster\*  
 King Abdullah University of Science and Technology

### SUMMARY

Standard migration images can suffer from migration artifacts due to 1) poor source-receiver sampling, 2) weak amplitudes caused by geometric spreading, 3) attenuation, 4) defocusing, 5) poor resolution due to limited source-receiver aperture, and 6) ringiness caused by a ringy source wavelet. To partly remedy these problems, least-squares migration (LSM), also known as linearized seismic inversion or migration deconvolution (MD), proposes to linearly invert seismic data for the reflectivity distribution. If the migration velocity model is sufficiently accurate, then LSM can mitigate many of the above problems and lead to a more resolved migration image, sometimes with twice the spatial resolution. However, there are two problems with LSM: the cost can be an order of magnitude more than standard migration and the quality of the LSM image is no better than the standard image for velocity errors of 5% or more. We now show how to get the most from least-squares migration by reducing the cost and velocity sensitivity of LSM.

### LEAST-SQUARES MIGRATION THEORY

The theory for least-squares migration is described in Nemeth et al. (1999) and Duquet et al. (2000), where the smooth background does not change with iteration number. Only the reflectivity distribution is updated at each iteration. This algorithm is equivalent to linearized waveform inversion (Lailly, 1984), and can be described as iteratively updating the reflectivity vector  $\mathbf{m}$  by

$$\mathbf{m}^{(k+1)} = \mathbf{m}^{(k)} - \alpha \mathbf{P} \mathbf{L}^T [\mathbf{L} \mathbf{m}^{(k)} - \mathbf{d}] + \text{regularization term}, \quad (1)$$

where  $\alpha$  is the step length,  $\mathbf{P}$  is the preconditioning matrix that approximates the inverse to the Hessian matrix,  $\mathbf{d}$  is the recorded reflection data,  $k$  represents the iteration index, and  $\mathbf{L}$  represents the linearized forward modeling operator that uses the smooth background velocity model<sup>1</sup>. If the preconditioner is inadequate, a conjugate gradient or quasi-Newton method is used to iteratively update the solution. In practice, the algorithm is often implemented in the time-space domain.

The implementation of LSM is described in Nemeth et al. (1999) and Duquet et al. (2000) for diffraction stack migration and in Plessix and Mulder (2004) for reverse time migration. Typically, diffraction stack migration provides images with fewer artifacts because it only smears reflections along the migration ellipses. In contrast, RTM automatically generates upgoing reflections from reflectors, so residuals are also smeared between

<sup>1</sup>A smooth velocity model is typically used so as to avoid smearing residuals along the rabbit-ear wavepaths. The smearing of residuals should only be along the migration ellipses that are tangent to the reflector boundaries (Zhan et al., 2014).

reflecting interfaces (Guitton, 2006; Liu et al., 2011; Zhan et al., 2014) to give rise to unwanted migration artifacts. To avoid such updates, we smooth the migration velocity model (McMechan, 1983; Loewenthal et al., 1987; Fletcher et al., 2005). To mitigate problems with an inaccurate migration velocity model, regularization terms or constraints (Sacchi et al., 2006; Guitton, 2006; Wang et al., 2011; Dong et al., 2012; Dai, 2013; Dai and Schuster, 2013) can be used to partly account for misaligned reflectors.

There are two different strategies for applying LSM to S distinct shot gathers (Dai et al., 2012; Dai and Schuster, 2013). The first strategy is to invert all of the shot gathers simultaneously for the reflectivity distribution, so this approach is denoted as overdetermined LSM (Dai, 2013). It is appropriate when the velocity model is accurate so the events in the common image gather are mostly aligned with one another. If there are significant errors in the velocity model, then the second approach is to invert shot gathers sequentially, and then stack together the prestack least-squares migration images. Prior to stacking, some type of regularization or trim statics can be applied to compensate for misaligned reflectors.

### Benefits of LSM

The benefits of LSM compared to standard migration are better spatial resolution, more uniform illumination of the subsurface, and reduction of aliasing artifacts due to coarse source-receiver sampling. Figure 1 depicts the migration images obtained by a) standard migration, and b) least-squares migration. The dashed box shows that there are fewer artifacts, better illumination, and greater resolution in the LSM image compared to the weak events in the RTM image.

If attenuation is present in the data, then amplitudes and higher frequencies in the migrated images become degraded with depth. However, a LSM method can be formulated that can partly account for attenuation loss if the Q-distribution is known (Dutta et al., 2013). If the modeling operator  $\mathbf{L}$  accounts for attenuation, then the Hessian inverse  $[\mathbf{L}^T \mathbf{L}]^{-1}$  estimated by iterative LSM partly compensates for the effects of attenuation suffered by the observed data  $\mathbf{d}$ . This requires an accurate estimate of the attenuation model as well as modeling and adjoint operators that account for anelastic effects (Blanch and Symes, 1995; Dutta et al., 2013).

Figure 3 shows the migration images for the Marmousi model with attenuation. The input data are generated by visco-acoustic modeling (see Robertsson et al., 1994) of the velocity and attenuation models, where the smoothed velocity model is used for migration. The Marmousi synthetic data are then migrated by Q-RTM and Q-LSRTM to give the images in Figures 3a and 3b, respectively. It is evident that Q-LSRTM with Q compensation correctly accounts for the attenuation loss when compared to Q-RTM, especially in the zoom views in Figure 4.

## Making the most of LSM

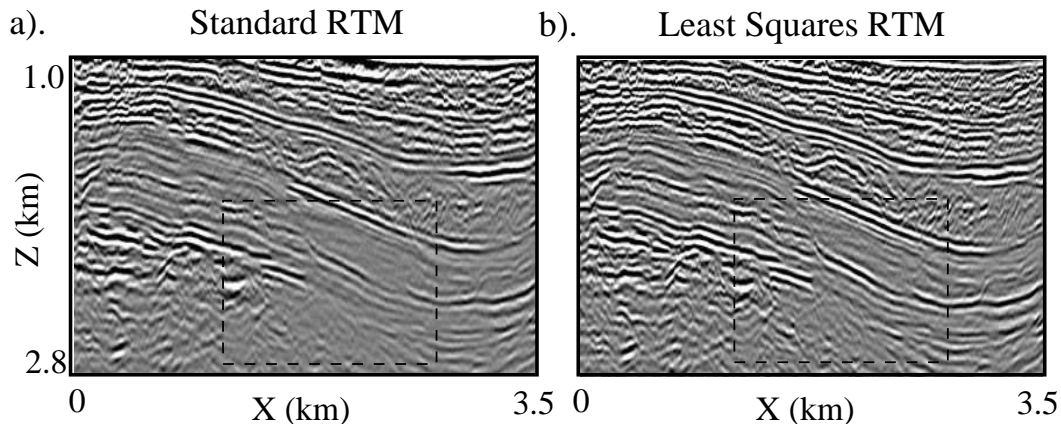


Figure 1: a) RTM, and b) least-squares reverse time migration (LSRTM) images computed from Gulf of Mexico data. The RTM image is computed by migrating and stacking each shot gather, while the LSRTM is computed with a normalized misfit function that matches the predicted phase with the recorded phase. There were 515 shot gathers with 480 receivers per shot, with a receiver (shot) interval of 37.5 m (12.5 m). The cable length is 6 km.

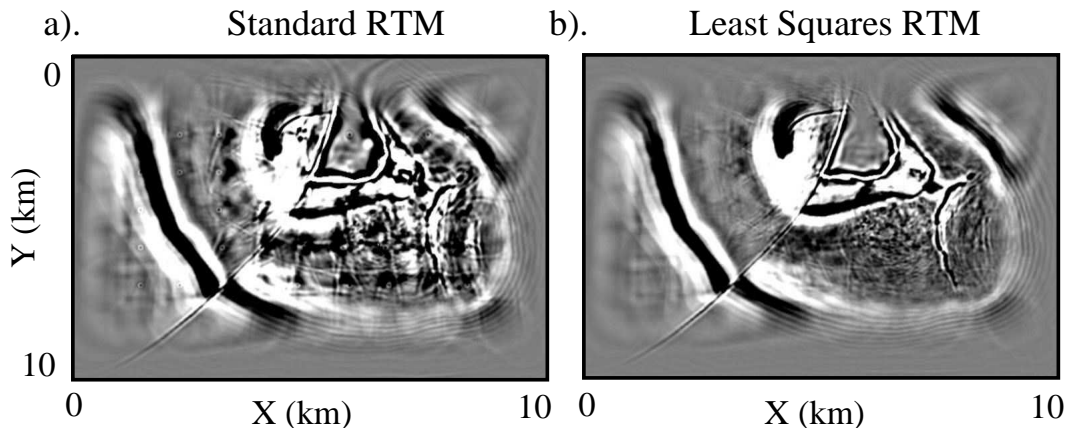


Figure 2: a) RTM, and b) LSRTM depth slices of migrated synthetic data associated with the SEG/EAGE salt model. There were 45 shot gathers, 200 receivers per shot, 9 shots on each sail line, and a total of 5 sail lines.

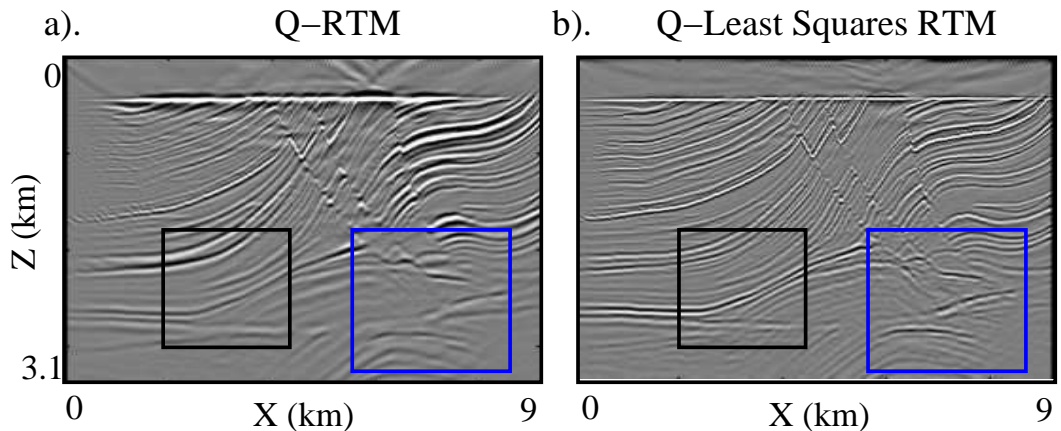


Figure 3: a) Q-RTM, and b) Q-Least Squares RTM images for the Marmousi model. The Q values were 20 between the depths of 0.5 and 2.0 km and 10000 elsewhere.

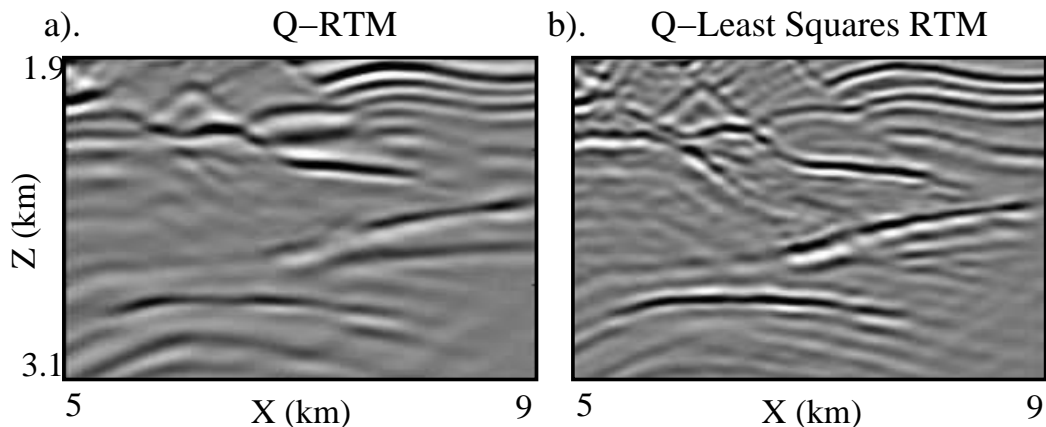


Figure 4: Zoom views of blue boxes in Figures 3a-b.

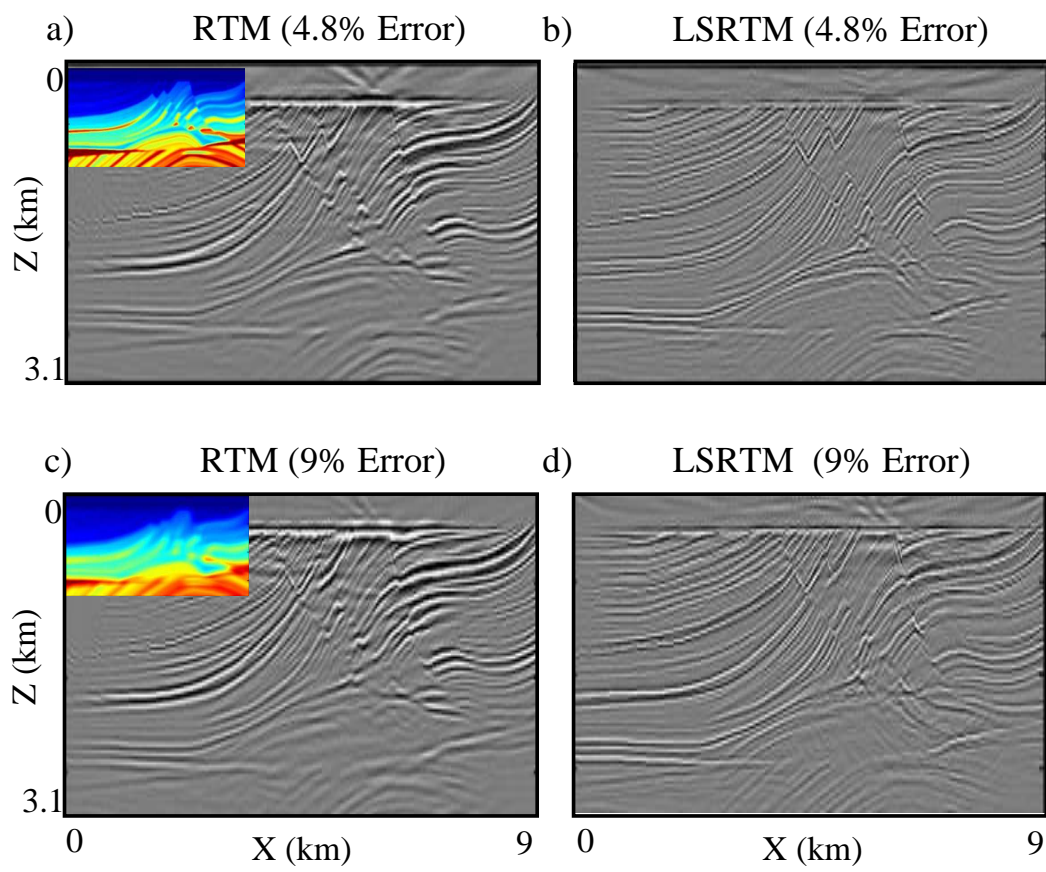


Figure 5: RTM and LSRTM images for (top row) 4.8% and (bottom row) 9.0% errors in the Marmousi velocity model. Insets are the Marmousi velocity model with errors

## Making the most of LSM

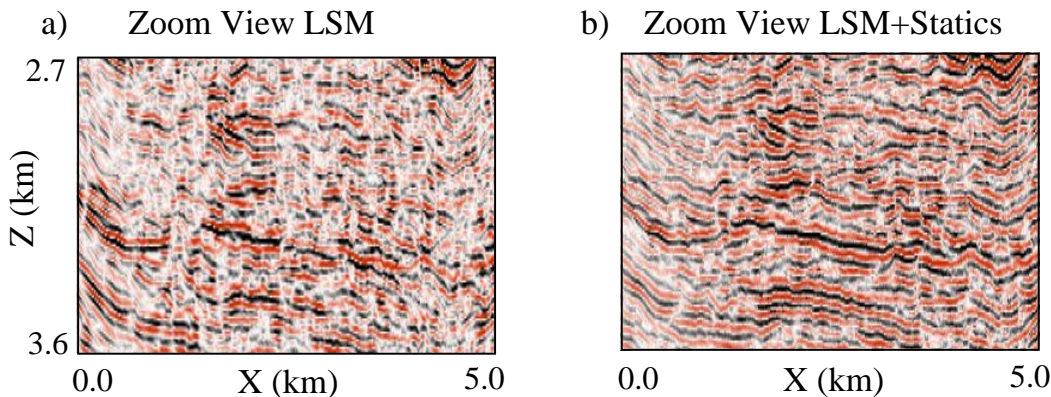


Figure 6: a) Conventional LSM and b) LSM+trim statics images after 10 iterations of LSM for 31 p-values of plane wave migration. The data set is recorded from a marine seismic survey in the Gulf of Mexico.

### PROBLEMS WITH LSM

The two most significant challenges with LSM are sensitivity to the accuracy of the migration velocity model and computational cost.

#### LSM Sensitivity to Velocity Errors

The migration velocity model must be accurate enough so that the events along a common horizon in the common image gather (CIG) are flattened to within a half wavelength of each other. Otherwise the stacked CIGs will be blurred and spoil the potential improvement in spatial resolution. See Figure 5 for an example. This suggests the need to combine a velocity inversion method such as migration velocity analysis (MVA), waveform inversion, traveltime tomography, or trim statics (Huang et al., 2014) to iteratively improve both the migration velocity and the reflectivity models.

#### Computational Cost of LSM

Least-squares migration is  $O(NX)$  times costlier than the 1X cost of standard migration, where  $N$  is the number of LSM iterations. To reduce the cost of wave equation LSM to acceptable levels, shot gathers can be encoded and blended together to form one supergather (Romero et al., 2000; Dai and Schuster, 2009; Tang and Biondi, 2009; Dai, 2012; Dai and Schuster, 2013). This means that just one encoded supergather needs to be migrated at each iteration, rather than sequentially migrating hundreds of shot gathers per iteration. There are at least five strategies for encoding the shot gathers and blending them into one supergather or several sub-supergathers. The benefit is to reduce the  $O(NX)$  cost of LSRTM to be anywhere from 8X to 0.1X the cost of standard RTM.

### TRIM STATICICS, LSM, AND VELOCITY UPDATES

If the common reflectors in two prestack migration images are misaligned in depth by more than one half of a wavelength for different shot gathers, then adding them together will lead to a smeared image. This will be true for both the overdetermined and the underdetermined migration images. To alleviate this

problem, a trim statics shift can be used to align the prestack migration images with one another prior to stack. The benefit is a more coherent migration image in the presence of inaccurate migration velocities, but the liability might be unacceptable positioning of the reflector image. The results shown in Figure 6 were obtained by applying trim statics to the prestack LSM images (Huang et al., 2014). It is quite evident that, for this example, the trim statics image is superior to the original image in terms of interface continuity. The statics shifts can be used to estimate the depth shift between common reflectors in different CIGs, and this depth residual can be used to update the velocity model (Stork, 1992).

### SUMMARY

The iterative least-squares migration method and its numerical implementation are described. Least-squares migration can provide reflectivity images with fewer migration artifacts, compensation for attenuation loss due to  $Q$ , and with higher spatial resolution than standard migration. In some cases, the spatial resolution of the LSM image can be more than twice that from standard migration, especially if  $Q$  compensation is provided. However, these improvements require a highly accurate migration velocity model so that the CIG reflection events along an interface are flattened to be within about 1/2 of a wavelength from one another. A sufficiently accurate velocity model can be obtained by MVA or some tomographic method such as full waveform inversion. Ideally, MVA and LSM should be combined so that both the velocity and reflectivity models are iteratively updated. The major cost barrier to wave equation LSM is largely eliminated by combining encoded shot gathers into either one supergather or several sub-supergathers. However, this cost reduction cannot be easily realized if trim statics and MVA are iteratively used to remedy defects due to inaccurate velocity models.

<http://dx.doi.org/10.1190/segam2014-1242.1>

#### EDITED REFERENCES

Note: This reference list is a copy-edited version of the reference list submitted by the author. Reference lists for the 2014 SEG Technical Program Expanded Abstracts have been copy edited so that references provided with the online metadata for each paper will achieve a high degree of linking to cited sources that appear on the Web.

#### REFERENCES

Blanch, J., and W. Symes, 1995, Efficient iterative viscoacoustic linearized inversion: 65<sup>th</sup> Annual International Meeting, SEG, Expanded Abstracts, **171**, 627–630.

Dai, W., 2012, Multisource least-squares reverse time migration: Ph.D. dissertation, King Abdullah University of Science and Technology.

Dai, W., C. Boonyasiriwat, and G. T. Schuster, 2010, 3D multisource least-squares reverse-time migration: 80<sup>th</sup> Annual International Meeting, SEG, Expanded Abstracts, **29**, 3120–3124, <http://dx.doi.org/10.1190/1.3513494>.

Dai, W., P. Fowler, and G. T. Schuster, 2012, Multisource least-squares reverse-time migration: Geophysical Prospecting, **60**, no. 4, 681–695, <http://dx.doi.org/10.1111/j.1365-2478.2012.01092.x>.

Dai, W., and G. Schuster, 2013, Plane-wave least-squares reverse-time migration: Geophysics, **78**, no. 4, S165–S177, <http://dx.doi.org/10.1190/geo2012-0377.1>.

Dai, W., and G. T. Schuster, 2009, Least-squares migration of simultaneous sources data with a deblurring filter: 79<sup>th</sup> Annual International Meeting, SEG, Expanded Abstracts, **600**, 2990–2994.

Dong, S., J. Cai, M. Guo, S. Suh, Z. Zhang, B. Wang, and Z. Li, 2012, Least-squares reverse-time migration: Toward true amplitude imaging and improving the resolution: Presented at the 82<sup>nd</sup> Annual International Meeting, SEG.

Duquet, B., K. J. Marfurt, and J. A. Dellingen, 2000, Kirchhoff modeling, inversion for reflectivity, and subsurface illumination: Geophysics, **65**, 1195–1209, <http://dx.doi.org/10.1190/1.1444812>.

Dutta, G., K. Lu, X. Wang, and G. T. Schuster, 2013, Attenuation compensation in least-squares reverse-time migration using the visco-acoustic wave equation: Presented at the 83<sup>rd</sup> Annual International Meeting, SEG.

Fletcher, R. F., P. Fowler, P. Kitchenside, and U. Albertin, 2005, Suppressing artifacts in prestack reverse-time migration: 75<sup>th</sup> Annual International Meeting, SEG, Expanded Abstracts, **522**, 2049–2051.

Guitton, A., B. Kaelin, and B. Biondi, 2006, Least-squares attenuation of reverse-time migration artifacts: 76<sup>th</sup> Annual International Meeting, SEG, Expanded Abstracts, **472**, 2348–2352.

Huang, Y., and G. T. Schuster, 2012, Multisource least-squares migration of marine streamer data with frequency-division encoding: Geophysical Prospecting, **60**, no. 4, 663–680, <http://dx.doi.org/10.1111/j.1365-2478.2012.01086.x>.

Huang, Y., X. Wang, and G. T. Schuster, 2014, Nonlocal means filter for trim statics: Presented at the 84<sup>th</sup> Annual International Meeting, SEG.

Lailly, P., 1984, Migration methods: partial but efficient solutions to the seismic inverse problem: Inverse Problems of Acoustic and Elastic Waves, **51**, 1387–1403.

Liu, F., G. Zhang, S. A. Morton, and J. P. Leveille, 2007, Reverse-time migration using one-way wavefield imaging condition: 77<sup>th</sup> Annual International Meeting, SEG, Expanded Abstracts, **439**, 2170–2174.

Loewenthal, D., P. Stoffa, and E. Faria, 1987, Suppressing the unwanted reflections of the full wave equations: *Geophysics*, **52**, 1007–1012, <http://dx.doi.org/10.1190/1.1442352>.

McMechan, G. A., 1983, Migration by extrapolation of time-dependent boundary values: *Geophysical Prospecting*, **31**, no. 3, 413–420, <http://dx.doi.org/10.1111/j.1365-2478.1983.tb01060.x>.

Nemeth, T., C. Wu, and G. T. Schuster, 1999, Least-squares migration of incomplete reflection data: *Geophysics*, **64**, 208–221, <http://dx.doi.org/10.1190/1.1444517>.

Plessix, R. E., and W. A. Mulder, 2004, Frequency-domain finite-difference amplitude-preserving migration: *Geophysical Journal International*, **157**, no. 3, 975–987, <http://dx.doi.org/10.1111/j.1365-246X.2004.02282.x>.

Robertsson, J., J. Blanch, and W. Symes, 1994, Viscoelastic finite-difference modelling: *Geophysics*, **59**, 1444–1456, <http://dx.doi.org/10.1190/1.1443701>.

Romero, L. A., D. C. Ghiglia, C. C. Ober, and S. A. Morton, 2000, Phase encoding of shot records in prestack migration: *Geophysics*, **65**, 426–436, <http://dx.doi.org/10.1190/1.1444737>.

Sacchi, M. D., J. Wang, and H. Kuehl, 2006, Regularized migration/inversion: new generation of imaging algorithms: *CSEG Recorder (Special Edition)*, **31**, 54–59.

Stork, C., 1992, Reflection tomography in the postmigrated domain: *Geophysics*, **57**, 680–692, <http://dx.doi.org/10.1190/1.1443282>.

Stork, C., and J. Kapoor, 2004, How many p-values do you want to migrate for delayed shot wave equation migration?: 74<sup>th</sup> Annual International Meeting, SEG, Expanded Abstracts, **262**, 1041–1044.

Tang, Y., 2009, Target-oriented wave-equation least-squares migration/inversion with phase-encoded Hessian: *Geophysics*, **74**, no. 6, WCA95–WCA107, <http://dx.doi.org/10.1190/1.3204768>.

Wang, J., and M. D. Sacchi, 2007, High-resolution wave-equation amplitude-variation-with-ray-parameter (AVP) imaging with sparseness constraints: *Geophysics*, **72**, no. 1, S11–S18, <http://dx.doi.org/10.1190/1.2387139>.

Wong, M., S. Ronen, and B. Biondi, 2011, Least-squares reverse-time migration/inversion for ocean bottom data: A case study: 81<sup>st</sup> Annual International Meeting, SEG, Expanded Abstracts, **30**, 2369–2373.

Zhan, G., W., Dai, Y., Luo, M., Zhou, and G.T. Schuster, 2014, Generalized diffraction-stack migration and filtering of coherent noise: *Geophysical Prospecting*, **62**, no. 3, 427–442, <http://dx.doi.org/10.1111/1365-2478.12086>.

Zhang, Y., L. Duan, and Y. Xie, 2013, A stable and practical implementation of least-squares reverse time migration: 83<sup>rd</sup> Annual International Meeting, SEG, Expanded Abstracts, doi: 10.1190/segam2013-0577.1.